NATIONAL ADVISORY COMMITTEE FOR AERONAUTICS

TECHNICAL NOTE

No. 1347

CRITICAL COMBINATIONS OF SHEAR AND LONGITUDINAL DIRECT STRESS FOR LONG PLATES WITH TRANSVERSE CURVATURE

By S. B. Batdorf, Murry Schildcrout, and Manuel Stein

Langley Memorial Aeronautical Laboratory
Langley Field, Va.

Washington
June 1947

NATIONAL ADVISORY COMMITTEE FOR AERONAUTICS

TECHNICAL NOTE NO. 1347

CRITICAL COMBINATIONS OF SHEAR AND LONGITUDINAL DIRECT STRESS FOR LONG PLATES WITH TRANSVERSE CURVATURE

By S. B. Batdorf, Murry Schildcrout, and Manuel Stein

SUMMARY

A theoretical solution is presented for the buckling stresses of long plates with transverse curvature loaded in shear and longitudinal direct stress. The theoretical critical-stress combinations for plates having either simply supported or clamped edges are given in figures and tables and a comparison is made with a previous theoretical solution for simply supported plates.

In the compression range theoretical curves are unsuitable for use in design because long plates with substantial curvature loaded in axial compression buckle at stresses that are much less than the theoretical values of critical stress. An investigation was therefore made to determine the modifications required to make the theoretical curves compatible with the available experimental data for plates in axial compression. Interaction curves based upon this investigation are provisionally recommended for use in design. Both theoretical and suggested design curves are essentially parabolas, a circumstance which permits simple approximate interaction formulas to be given.

INTRODUCTION

Theoretical solutions to a number of problems concerned with the determination of the critical stresses which cause long curved plates to buckle have been presented in various investigations. In references 1 to 3 shear alone acting on both simply supported and clamped plates is investigated; in references 4 and 5 direct axial compression alone acting on both simply supported and clamped plates is investigated; and in reference 6 the critical combinations of shear and direct axial stress for simply supported plates only are given.

The present paper deals with the determination of the combinations of shear and direct axial stress which cause plates with either

simply supported or clamped edges to buckle (appendix A). The present solution as well as the solutions of references 1 to 6 is based upon the small-deflection theory. As curved plates loaded in axial compression may buckle at a stress much less than the theoretical value, the theoretical interaction curves of reference 6 and the present paper must be modified in the compression range for use in design.

An investigation was therefore made of available experimental data on the critical stresses of long plates with transverse curvature loaded in axial compression (appendix B), and approximate interaction curves incorporating these results were developed and are provisionally recommended for design purposes. The results of the present analysis are given in the form of tables, interaction curves, and formulas.

SYMBOLS

b	width of plate
m, n, j	integers
r	radius of curvature of plate
t	thickness of plate
u	displacement of point on median surface of plate in axial (x-) direction
v	displacement of point on median surface of plate in circumferential (y-) direction
w	displacement of point on median surface of plate in radial direction; positive outward
x	axial coordinate of plate
y	circumferential coordinate of plate
D	flexural stiffness of plate per unit length $\left(\frac{Et^3}{12(1-\mu^2)}\right)$
E	Young's modulus of elasticity
Q	mathematical operator defined in appendix A

Z curvature parameter $\left(\frac{b^2}{rt}\sqrt{1-\mu^2} \text{ or } \left(\frac{b}{r}\right)^2 \frac{r}{t}\sqrt{1-\mu^2}\right)$

a_n, b_n coefficients of deflection functions

k_s shear-stress coefficient appearing in equation $\tau = \frac{k_s \pi^2 D}{b^2 t}$

k_x direct-axial-stress coefficient appearing in equation $\sigma_x = \frac{k_x \pi^2 D}{b^2 t}$

M_n diagonal element in stability determinant

$(R_s)_{th}$ theoretical shear-stress ratio (ratio of shear stress present to theoretical critical shear stress in absence of other stresses)

$(R_x)_{exp}$ empirical direct-axial-stress ratio (ratio of direct axial stress present to empirical critical direct axial stress in absence of other stresses)

$(R_x)_{th}$ theoretical direct-axial-stress ratio (ratio of direct axial stress present to theoretical direct axial stress in absence of other stresses)

V_m, W_m deflection functions defined in appendix A

$\beta = \frac{b}{\lambda}$

λ half wave length of buckles in axial direction

μ Poisson's ratio

σ_x direct axial stress in plate

τ shear stress in plate

$$\nabla^4 = \frac{\partial^4}{\partial x^4} + 2\frac{\partial^4}{\partial x^2 \partial y^2} + \frac{\partial^4}{\partial y^4}$$

∇^{-4} = inverse of ∇^4, defined by $\nabla^{-4}\left(\nabla^4 w\right) = w$

RESULTS AND DISCUSSION

Thoeretical results.- The combinations of shear and axial stress which cause long plates with transverse curvature to buckle may be obtained from the equations

$$\tau = \frac{k_s \pi^2 D}{b^2 t}$$

$$\sigma_x = \frac{k_x \pi^2 D}{b^2 t}$$

when the stress coefficients k_s and k_x are known. The theoretical combinations of stross coefficients for plates with simply supported edges and clamped edges are given by the interaction curves of figures 1 and 2, respectively. In these figures, the dashed curves for $Z = 0$ are flat-plate solutions obtained from reference 7.

In figures 1 and 2 interaction curves are presented for various values of the curvature parameter Z up to 30. The interaction curves are very nearly parabolas passing through the points giving the critical stress coefficients for shear alone and for axial stress alone. These stress coefficients for any value of Z may be obtained from the theoretical curves of figures 3 and 4, which incorporate results derived in reference 3 and in appendix A of the present paper. Additional calculations made for curved plates both with simply supported and with clamped edges indicate that for all values of Z up to at least 1000 the interaction curves continue to be approximately parabolas (computed values given in table 1). These results are confirmed for simply supported plates by the results given in reference 6.

Empirical results and design curves.- Reference 8 shows that curved plates in shear buckle at stresses close to the theoretical

critical stresses. Plates of moderate or high curvature in axial compression, however, buckle at stresses much less than the theoretical critical stresses. (See references 9 to 11.) The theoretical interaction curves are therefore seriously unconservative for plates of moderate or high curvature when appreciable compression is present and are thus unsuitable for use in the design of such plates. This discrepancy between the actual and the theoretical compressive stresses is believed to be due to nonlinear effects which are not accounted for in the small-deflection theory. The fraction of the theoretical critical stress at which these effects assume importance depends upon the initial eccentricities of the plate.

Because the ratio r/t is a rough measure of the initial eccentricities likely to be present in practical construction, the available experimental critical compressive stresses were plotted in separate groups according to the value of r/t of the plate and a separate curve was faired through each group. (See appendix B.) The results are summarized in figure 5. The empirical curves have the same general trend as the theoretical curves and at high values of Z approach straight lines given approximately by the formula

$$k_x = \left(0.68 - 0.0005\frac{r}{t}\right)Z$$

for values of r/t between 500 and 1000. (See appendix B.)

The true interaction curve for a given curved plate must pass through the experimental point for pure compression, which can be obtained from figure 5, and also through the experimental point for pure shear, which falls slightly below the theoretical value indicated in figure 3. Because the small-deflection theory gives fairly accurate results except in the presence of substantial axial compression (reference 12), the theoretical curve must be approximately correct in the tension and part of the compression range. The true interaction curve is therefore presumably somewhat like the dashed curve in figure 6. The absence of experimental data does not permit accurate plotting of this curve; therefore an approximate design curve consisting of two parts (as indicated in fig. 6) is suggested. One part, applying to the compression range, is the parabola passing through the points corresponding to the experimental critical compressive stress and the theoretical critical shear stress (obtained from figs. 5 and 3, respectively). The second part, applying to the tension range, is the theoretical curve which is essentially the parabola passing through the points corresponding to the theoretical

critical stress in pure compression and pure shear (obtained from figs. 4 and 3, respectively).

INTERACTION FORMULAS

The theoretical interaction curve for a long plate with transverse curvature loaded in shear and longitudinal direct stress is very nearly a parabola passing through the theoretical points corresponding to shear alone and to axial compression alone. This parabola may be expressed in stress-ratio form by the equation

$$\left(R_s\right)_{th}^2 + \left(R_x\right)_{th} = 1$$

As long plates with transverse curvature in axial compression buckle at a stress considerably less than the theoretical critical stress, the theoretical interaction curve is unsuitable for design purposes whenever a substantial amount of compression is present. In the absence of test data on curved plates buckling under combined shear and compression, an interaction curve composed of two parts is provisionally recommended for design. This interaction curve is described by the following equations: For combined shear and compression,

$$\left(R_s\right)_{th}^2 + \left(R_x\right)_{exp} = 1$$

and for combined shear and tension,

$$\left(R_s\right)_{th}^2 + \left(R_x\right)_{th} = 1$$

Langley Memorial Aeronautical Laboratory
National Advisory Committee for Aeronautics
Langley Field, Va., March 20, 1947

APPENDIX A

THEORETICAL SOLUTION

Equation of equilibrium.- The combinations of shear and direct axial stress which cause long curved plates to buckle may be obtained by solving the following equation of equilibrium (reference 13):

$$D\nabla^4 w + \frac{Et}{r^2}\nabla^{-4}\frac{\partial^4 w}{\partial x^4} + 2\tau t\frac{\partial^2 w}{\partial x\,\partial y} + \sigma_x t\frac{\partial^2 w}{\partial x^2} = 0 \qquad (A1)$$

where x and y are the coordinates indicated in the following figure:

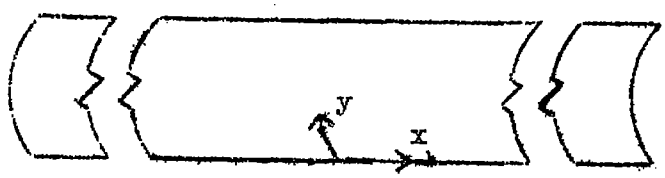

Division of equation (A1) by D gives

$$\nabla^4 w + \frac{12Z^2}{b^4}\nabla^{-4}\frac{\partial^4 w}{\partial x^4} + 2k_s\frac{\pi^2}{b^2}\frac{\partial^2 w}{\partial x\,\partial y} + k_x\frac{\pi^2}{b^2}\frac{\partial^2 w}{\partial x^2} = 0 \qquad (A2)$$

where the dimensionless parameters Z, k_s, and k_x are defined by

$$Z = \frac{b^2}{rt}\sqrt{1 - \mu^2}$$

$$k_s = \frac{\tau t b^2}{\pi^2 D}$$

$$k_x = \frac{\sigma_x t b^2}{\pi^2 D}$$

Equation (A2) can be represented by

$$Qw = 0 \tag{A3}$$

where Q is defined by the operator

$$\nabla^4 + \frac{12Z^2}{b^4}\nabla^{-4}\frac{\partial^4}{\partial x^4} + 2k_s\frac{\pi^2}{b^2}\frac{\partial^2}{\partial x\,\partial y} + k_x\frac{\pi^2}{b^2}\frac{\partial^2}{\partial x^2}$$

Method of solution.- The equation of equilibrium may be solved by using the Galerkin method as given in reference 14. In the application of this method, equation (A3) is solved by the use of a suitable series expansion for w as follows:

$$w = \sum_{m=1}^{j} a_m V_m + \sum_{m=1}^{j} b_m W_m \tag{A4}$$

In expression (A4) the functions $V_1, V_2, \ldots V_j$, and $W_1, W_2, \ldots W_j$ individually satisfy the boundary conditions on w but need not satisfy

the equation of equilibrium. The coefficients a_m and b_m are then determined by the equations

$$\left.\begin{aligned} \int_0^b \int_0^{2\lambda} V_n Q w \, dx \, dy = 0 \\ \int_0^b \int_0^{2\lambda} W_n Q w \, dx \, dy = 0 \end{aligned}\right\} \tag{A5}$$

where $n = 1, 2, 3, \ldots j$.

The boundary conditions considered in the present paper are as follows: for simply supported edges, $w = \frac{\partial^2 w}{\partial y^2} = u = 0$ and v is unrestrained; and for clamped edges, $w = \frac{\partial w}{\partial y} = v = 0$ and u is unrestrained.

Solution for plates with simply supported edges.- The following infinite series expansion, which incorporates a set of functions that is complete (subject to the limitation of periodicity with wave length 2λ in the longitudinal direction), can be used to represent exactly the displacement w of curved plates with simply supported edges:

$$w = \sin \frac{\pi x}{\lambda} \sum_{m=1}^{\infty} a_m \sin \frac{m\pi y}{b} + \cos \frac{\pi x}{\lambda} \sum_{m=1}^{\infty} b_m \sin \frac{m\pi y}{b} \tag{A6}$$

In addition to satisfying the conditions on w at the edges, expression (A6) also satisfies the conditions that the axial displacement u is equal to 0 and the circumferential displacement v is unrestrained at the edges (see reference 12). Expression (A6) is equivalent to expression (A4) if

$$\left.\begin{aligned} V_n &= \sin\frac{\pi x}{\lambda}\sin\frac{n\pi y}{b} \\ W_n &= \cos\frac{\pi x}{\lambda}\sin\frac{n\pi y}{b} \end{aligned}\right\} \tag{A7}$$

Substitution of expressions (A6) and (A7) into equations (A5) and integration over the limits indicated give

$$\left.\begin{aligned} a_n\left[\left(n^2+\beta^2\right)^2+\frac{12Z^2\beta^4}{\pi^4\left(n^2+\beta^2\right)^2}-k_x\beta^2\right]-\frac{8k_s\beta}{\pi}\sum_{m=1}^{\infty}b_m\frac{mn}{n^2-m^2}=0 \\ b_n\left[\left(n^2+\beta^2\right)^2+\frac{12Z^2\beta^4}{\pi^4\left(n^2+\beta^2\right)^2}-k_x\beta^2\right]+\frac{8k_s\beta}{\pi}\sum_{m=1}^{\infty}a_m\frac{mn}{n^2-m^2}=0 \end{aligned}\right\} \tag{A8}$$

where $m \pm n$ is odd and

$$\beta = \frac{b}{\lambda}$$

$n = 1, 2, 3, \ldots$

Equations (A8) have a solution in which the coefficients a_n and the coefficients b_n are not all zero only if the following determinant of the coefficients of a_n and b_n vanishes:

	a_1	a_2	a_3	a_4	a_5	a_6	...	b_1	b_2	b_3	b_4	b_5	b_6	...
n=1	$\frac{1}{k_s}M_1$	0	0	0	0	0	...	0	$\frac{2}{3}$	0	$\frac{4}{15}$	0	$\frac{6}{35}$	...
n=2	0	$\frac{1}{k_s}M_2$	0	0	0	0	...	$-\frac{2}{3}$	0	$\frac{6}{5}$	0	$\frac{10}{21}$	0	...
n=3	0	0	$\frac{1}{k_s}M_3$	0	0	0	...	0	$-\frac{6}{5}$	0	$\frac{12}{7}$	0	$\frac{2}{3}$	...
n=4	0	0	0	$\frac{1}{k_s}M_4$	0	0	...	$-\frac{4}{15}$	0	$-\frac{12}{7}$	0	$\frac{20}{9}$	0	...
n=5	0	0	0	0	$\frac{1}{k_s}M_5$	0	...	0	$-\frac{10}{21}$	0	$-\frac{20}{9}$	0	$\frac{30}{11}$	...
n=6	0	0	0	0	0	$\frac{1}{k_s}M_6$	...	$-\frac{6}{35}$	0	$-\frac{2}{3}$	0	$-\frac{30}{11}$	0	...
.	.	.	.	.	.	.	.	.	.	.	.	.	.	.
.	.	.	.	.	.	.	.	.	.	.	.	.	.	.
.	.	.	.	.	.	.	.	.	.	.	.	.	.	.
n=1	0	$-\frac{2}{3}$	0	$-\frac{4}{15}$	0	$-\frac{6}{35}$	...	$\frac{1}{k_s}M_1$	0	0	0	0	0	...
n=2	$\frac{2}{3}$	0	$-\frac{6}{5}$	0	$-\frac{10}{21}$	0	...	0	$\frac{1}{k_s}M_2$	0	0	0	0	...
n=3	0	$\frac{6}{5}$	0	$-\frac{12}{7}$	0	$-\frac{2}{3}$	...	0	0	$\frac{1}{k_s}M_3$	0	0	0	...
n=4	$\frac{4}{15}$	0	$\frac{12}{7}$	0	$-\frac{20}{9}$	0	...	0	0	0	$\frac{1}{k_s}M_4$	0	0	...
n=5	0	$\frac{10}{21}$	0	$\frac{20}{9}$	0	$-\frac{30}{11}$	...	0	0	0	0	$\frac{1}{k_s}M_5$	0	...
n=6	$\frac{6}{35}$	0	$\frac{2}{3}$	0	$\frac{30}{11}$	0	...	0	0	0	0	0	$\frac{1}{k_s}M_6$	...
.	.	.	.	.	.	.	.	.	.	.	.	.	.	.
.	.	.	.	.	.	.	.	.	.	.	.	.	.	.
.	.	.	.	.	.	.	.	.	.	.	.	.	.	.

(A9)

where

$$M_n = \frac{\pi}{8\beta}\left[\left(n^2+\beta^2\right)^2 + \frac{12\beta^4}{\pi^4}\frac{Z^2}{\left(n^2+\beta^2\right)^2} - k_x\beta^2\right]$$

By a rearrangement of rows and columns, the infinite determinant can be factored into the product of two mutually equivalent infinite subdeterminants. The resulting equation, which determines the critical stress combinations, is

$$\begin{vmatrix}
 & a_1 & b_2 & a_3 & b_4 & a_5 & b_6 & \cdots & b_1 & a_2 & b_3 & a_4 & b_5 & a_6 & \cdots \\
n=1 & \frac{1}{k_s}M_1 & \frac{2}{3} & 0 & \frac{4}{15} & 0 & \frac{6}{35} & \cdots & 0 & 0 & 0 & 0 & 0 & 0 & \cdots \\
n=2 & \frac{2}{3} & \frac{1}{k_s}M_2 & -\frac{6}{5} & 0 & -\frac{10}{21} & 0 & \cdots & 0 & 0 & 0 & 0 & 0 & 0 & \cdots \\
n=3 & 0 & -\frac{6}{5} & \frac{1}{k_s}M_3 & \frac{12}{7} & 0 & \frac{2}{3} & \cdots & 0 & 0 & 0 & 0 & 0 & 0 & \cdots \\
n=4 & \frac{4}{15} & 0 & \frac{12}{7} & \frac{1}{k_s}M_4 & -\frac{20}{9} & 0 & \cdots & 0 & 0 & 0 & 0 & 0 & 0 & \cdots \\
n=5 & 0 & -\frac{10}{21} & 0 & -\frac{20}{9} & \frac{1}{k_s}M_5 & \frac{30}{11} & \cdots & 0 & 0 & 0 & 0 & 0 & 0 & \cdots \\
n=6 & \frac{6}{35} & 0 & \frac{2}{3} & 0 & \frac{30}{11} & \frac{1}{k_s}M_6 & \cdots & 0 & 0 & 0 & 0 & 0 & 0 & \cdots \\
\vdots & \vdots & \vdots & \vdots & \vdots & \vdots & \vdots & \vdots & \vdots & \vdots & \vdots & \vdots & \vdots & \vdots & \vdots \\
n=1 & 0 & 0 & 0 & 0 & 0 & 0 & \cdots & \frac{1}{k_s}M_1 & -\frac{2}{3} & 0 & -\frac{4}{15} & 0 & -\frac{6}{35} & \cdots \\
n=2 & 0 & 0 & 0 & 0 & 0 & 0 & \cdots & -\frac{2}{3} & \frac{1}{k_s}M_2 & \frac{6}{5} & 0 & \frac{10}{21} & 0 & \cdots \\
n=3 & 0 & 0 & 0 & 0 & 0 & 0 & \cdots & 0 & \frac{6}{5} & \frac{1}{k_s}M_3 & -\frac{12}{7} & 0 & -\frac{2}{3} & \cdots \\
n=4 & 0 & 0 & 0 & 0 & 0 & 0 & \cdots & -\frac{4}{15} & 0 & -\frac{12}{7} & \frac{1}{k_s}M_4 & \frac{20}{9} & 0 & \cdots \\
n=5 & 0 & 0 & 0 & 0 & 0 & 0 & \cdots & 0 & \frac{10}{21} & 0 & \frac{20}{9} & \frac{1}{k_s}M_5 & -\frac{30}{11} & \cdots \\
n=6 & 0 & 0 & 0 & 0 & 0 & 0 & \cdots & -\frac{6}{35} & 0 & -\frac{2}{3} & 0 & -\frac{30}{11} & \frac{1}{k_s}M_6 & \cdots \\
\vdots & \vdots & \vdots & \vdots & \vdots & \vdots & \vdots & \vdots & \vdots & \vdots & \vdots & \vdots & \vdots & \vdots & \vdots
\end{vmatrix} = 0 \qquad \text{(A10)}$$

The first approximation, obtained from the second-order determinant (upper left-hand corner of either of the infinite subdeterminants), is given by

$$k_s^2 = \frac{9}{4}M_1M_2 \tag{A11}$$

The second approximation, obtained from the third-order determinant, is given by

$$k_s^2 = \frac{M_1M_2M_3}{\frac{36}{25}M_1 + \frac{4}{9}M_3} \tag{A12}$$

The third approximation, obtained from the fourth-order determinant, is given by

$$k_s^4\left(\frac{8}{7}+\frac{8}{25}\right)^2 - k_s^2\left(\frac{144}{49}M_1M_2+\frac{36}{25}M_1M_4+\frac{16}{225}M_2M_3+\frac{4}{9}M_3M_4\right)+M_1M_2M_3M_4 = 0 \tag{A13}$$

Each of these equations shows that for a selected value of the curvature parameter Z the critical combination of stresses which will cause a long curved plate to buckle depends upon the wave length. Since a structure buckles at the lowest stress at which instability can occur, k_s is minimized with respect to the wave length by substituting values of β into equations (A11), (A12), or (A13) for a chosen value of k_x until the minimum value of k_s can be obtained from a plot of k_s against β. Table 1 presents the computed interaction data; the results are substantially the same as the results of reference 6.

In order to determine the critical stress coefficients for the buckling of a long curved plate loaded in axial compression alone, equation (A10) is solved by setting k_s equal to zero. In the resultant equation all the off-diagonal terms are equal to zero. The solution to this equation is

$$M_1M_2M_3 \cdot \cdot \cdot M_n = 0 \tag{A14}$$

For the minimum value of the stress coefficient that satisfies equation (A14), the relationship

$$M_1 = 0 \tag{A15}$$

must be satisfied. The value of k_x given by equation (A15) is

$$k_x = \frac{(\beta^2 + 1)^2}{\beta^2} + \frac{12Z^2\beta^2}{\pi^4(\beta^2 + 1)^2} \tag{A16}$$

Equation (A16) shows that the buckling stress is a function of the wave length of the buckle and the minimum value of k_x is found by minimizing k_x with respect to β in a manner similar to that used to find the minimum value of k_s in equations (A11) to (A13). Figure 4 gives the critical axial-compressive-stress coefficients for long curved plates with simply supported edges; the results are the same as the results presented in reference 4 for plates with simply supported edges.

Solution for plates with clamped edges.- A procedure similar to that used for plates with simply supported edges may be followed for long curved plates with clamped edges. The deflection function used is the following series:

$$w = \sin\frac{\pi x}{\lambda}\sum_{m=1}^{\infty} a_m\left[\cos\frac{(m-1)\pi y}{b} - \cos\frac{(m+1)\pi y}{b}\right]$$

$$+ \cos\frac{\pi x}{\lambda}\sum_{m=1}^{\infty} b_m\left[\cos\frac{(m-1)\pi y}{b} - \cos\frac{(m+1)\pi y}{b}\right] \tag{A17}$$

Each term of this series satisfies the conditions on w at the edges and in addition the conditions that the axial displacement u is unrestrained and the circumferential displacement v is equal to 0 at the edges (see reference 13). In this case,

$$\left.\begin{aligned} V_n &= \sin\frac{\pi x}{\lambda}\left[\cos\frac{(n-1)\pi y}{b} - \cos\frac{(n+1)\pi y}{b}\right] \\ W_n &= \cos\frac{\pi x}{\lambda}\left[\cos\frac{(n-1)\pi y}{b} - \cos\frac{(n+1)\pi y}{b}\right] \end{aligned}\right\} \quad \text{(A18)}$$

where $n = 1, 2, 3 \ldots$

After operations corresponding to those carried out for the case of simply supported edges are performed, the following simultaneous equations result:

For $n = 1$

$$a_1(2M_0 + M_2) - a_3M_2 + k_s \sum_{m=2,4,6}^{\infty} b_m\left[\frac{-(m-1)^2}{(m-1)^2-4} + \frac{(m+1)^2}{(m+1)^2-4}\right] = 0$$

For $n = 2$

$$a_2(M_1 + M_3) - a_4M_3 + k_s \sum_{m=1,3,5}^{\infty} b_m\left[\frac{(m-1)^2}{(m-1)^2-1} - \frac{(m-1)^2}{(m-1)^2-9} - \frac{(m+1)^2}{(m+1)^2-1} + \frac{(m+1)^2}{(m+1)^2-9}\right] = 0$$

For $n = 3, 4, 5, \ldots$

$$a_n(M_{n-1} + M_{n+1}) - a_{n-2}M_{n-1} - a_{n+2}M_{n+1} + k_s \sum_{m=1}^{\infty} b_m\left[\frac{(m-1)^2}{(m-1)^2-(n-1)^2} - \frac{(m-1)^2}{(m-1)^2-(n+1)^2} - \frac{(m+1)^2}{(m+1)^2-(n-1)^2} + \frac{(m+1)^2}{(m+1)^2-(n+1)^2}\right] = 0$$

where $m \pm n$ is odd.

For $n = 1$

$$b_1(2M_0 + M_2) - b_3M_2 - k_s \sum_{m=2,4,6}^{\infty} a_m\left[\frac{-(m-1)^2}{(m-1)^2-4} + \frac{(m+1)^2}{(m+1)^2-4}\right] = 0$$

For $n = 2$

$$b_2(M_1 + M_3) - b_4M_3 - k_s \sum_{m=1,3,5}^{\infty} a_m\left[\frac{(m-1)^2}{(m-1)^2-1} - \frac{(m-1)^2}{(m-1)^2-9} - \frac{(m+1)^2}{(m+1)^2-1} + \frac{(m+1)^2}{(m+1)^2-9}\right] = 0$$

For $n = 3, 4, 5, \ldots$

$$b_n(M_{n-1} + M_{n+1}) - b_{n-2}M_{n-1} - b_{n+2}M_{n+1} - k_s \sum_{m=1}^{\infty} a_m\left[\frac{(m-1)^2}{(m-1)^2-(n-1)^2} - \frac{(m-1)^2}{(m-1)^2-(n+1)^2} - \frac{(m+1)^2}{(m+1)^2-(n-1)^2} + \frac{(m+1)^2}{(m+1)^2-(n+1)^2}\right] = 0$$

where $m \pm n$ is odd

(A19)

and

$$M_n = \frac{\pi}{8\beta}\left[\left(n^2+\beta^2\right)^2 + \frac{12Z^2\beta^4}{\pi^4\left(n^2+\beta^2\right)^2} - k_x\beta^2\right]$$

The infinite determinant formed by equations (A19) can be rearranged so as to factor into the product of two mutually equivalent infinite subdeterminants, as in the solution for long curved plates with simply supported edges. The critical stress combinations are obtained by permitting one of the subdeterminants to vanish. The resultant equation is

$$\begin{array}{c|cccccc|} & a_1 & b_2 & a_3 & b_4 & a_5 & b_6 & \cdots \\ n=1 & \frac{1}{k_s}\left(2M_0+M_2\right) & \frac{32}{15} & -\frac{1}{k_s}M_2 & -\frac{64}{105} & 0 & -\frac{32}{315} & \cdots \\ n=2 & \frac{32}{15} & \frac{1}{k_s}\left(M_1+M_3\right) & -\frac{352}{105} & -\frac{1}{k_s}M_3 & \frac{32}{35} & 0 & \cdots \\ n=3 & -\frac{1}{k_s}M_2 & -\frac{352}{105} & \frac{1}{k_s}\left(M_2+M_4\right) & \frac{1472}{315} & -\frac{1}{k_s}M_4 & -\frac{1376}{1155} & \cdots \\ n=4 & -\frac{64}{105} & -\frac{1}{k_s}M_3 & \frac{1472}{315} & \frac{1}{k_s}\left(M_3+M_5\right) & -\frac{4160}{693} & -\frac{1}{k_s}M_5 & \cdots \\ n=5 & 0 & \frac{32}{35} & -\frac{1}{k_s}M_4 & -\frac{4160}{693} & \frac{1}{k_s}\left(M_4+M_6\right) & \frac{9440}{1287} & \cdots \\ n=6 & -\frac{32}{315} & 0 & -\frac{1376}{1155} & -\frac{1}{k_s}M_5 & \frac{9440}{1287} & \frac{1}{k_s}\left(M_5+M_7\right) & \cdots \\ \vdots & \vdots & \vdots & \vdots & \vdots & \vdots & \vdots & \\ \vdots & \vdots & \vdots & \vdots & \vdots & \vdots & \vdots & \\ \vdots & \vdots & \vdots & \vdots & \vdots & \vdots & \vdots & \end{array} = 0 \qquad \text{(A20)}$$

The first approximation to equation (A20), obtained from the second-order determinant (upper left-hand corner of equation (A20)), is given by

$$k_s^2 = \left(\frac{15}{32}\right)^2 (2M_0 + M_2)(M_1 + M_3) \tag{A21}$$

The second approximation, obtained from the third-order determinant, is given by

$$k_s^2 = \frac{(M_1 + M_3)\left[2(2M_0 + M_2)(M_2 + M_4) - M_2^2\right]}{\left(\frac{32}{15}\right)^2 (M_2 + M_4) - \left(\frac{64}{15}\right)\left(\frac{352}{105}\right)M_2 + \left(\frac{352}{105}\right)^2 (2M_0 + M_2)} \tag{A22}$$

The third approximation, obtained from the fourth-order determinant, is given by

$$\begin{aligned} k_s^4 &\left[\left(\frac{32}{15}\right)\left(\frac{1472}{315}\right) - \left(\frac{352}{105}\right)\left(\frac{64}{105}\right)\right]^2 - k_s^2 \left\{\left(\frac{1472}{315}\right)^2 (2M_0 + M_2)(M_1 + M_3)\right. \\ &+ \left(\frac{352}{105}\right)^2 (2M_0 + M_2)(M_3 + M_5) + \left(\frac{64}{105}\right)^2 (M_1 + M_3)(M_2 + M_4) \\ &+ \left(\frac{32}{15}\right)^2 (M_2 + M_4)(M_3 + M_5) - \left(\frac{128}{105}\right)\left(\frac{1472}{315}\right)M_2(M_1 + M_3) \\ &- \left(\frac{64}{15}\right)\left(\frac{352}{105}\right)M_2(M_3 + M_5) - \left(\frac{704}{105}\right)\left(\frac{1472}{315}\right)M_3(2M_0 + M_2) \\ &\left. - \left(\frac{64}{15}\right)\left(\frac{64}{105}\right)M_3(M_2 + M_4) + \left[\left(\frac{128}{105}\right)\left(\frac{352}{105}\right) + \left(\frac{64}{15}\right)\left(\frac{1472}{315}\right)\right]M_2M_3\right\} \\ &+ \left[2M_0(M_2 + M_4) + M_2M_4\right]\left[M_1(M_3 + M_5) + M_3M_5\right] = 0 \end{aligned} \tag{A23}$$

These equations are solved for values of Z between 0 and 30 in a manner similar to that used in the problem of the buckling of curved plates with simply supported edges - that is, by substituting values of β into equations (A21), (A22), or (A23) for each value of Z and a given value of k_x until the minimum value of k_s is obtained from a plot of β against corresponding values of k_s. As the value of Z increases, the higher Fourier components of the buckle deformation increase in relative importance, and instead of determinants in the upper left-hand corner determinants farther down the principal diagonal are used. The computed interaction data are presented in table 1.

In order to determine the critical stress coefficients for the buckling of a long curved plate in axial compression, equation (A23) is solved by setting k_s equal to zero. The solution then is

$$\left[2M_0\left(M_2 + M_4\right) + M_2M_4\right]\left[M_1\left(M_3 + M_5\right) + M_3M_5\right] = 0 \qquad (A24)$$

Equation (A24) is solved in a manner similar to that used for the problem of the buckling of a curved plate with simply supported edges under axial compression - that is, by substituting values of β into equation (A24) until the minimum value of k_x is found from a plot of k_x against β. Figure 4 gives the critical axial-compressive-stress coefficients for long curved plates with clamped edges, and these values are in substantial agreement with the results presented in reference 5 for plates of low curvature with clamped edges.

APPENDIX B

DETERMINATION OF EMPIRICAL CURVES FOR BUCKLING OF LONG PLATES WITH TRANSVERSE CURVATURE LOADED IN AXIAL COMPRESSION

Curved plates loaded in axial compression buckle at loads which are much lower than those predicted by theory (see references 9 to 11). In order to determine the loads at which actual curved plates would buckle an empirical investigation was carried out.

When plates have appreciable curvature, the critical compressive stresses are virtually independent of the ratio of the axial length to the circumferential width of the plates, if this ratio is greater than about 1. The test data obtained in various investigations for the buckling of curved rectangular panels having a ratio of axial length to circumferential width greater than 1 were plotted in figures 7 and 8 by using the parameters of the small-deflection theory. These figures show that as the radius-thickness ratio of the plates increases the buckling stresses decrease. A series of curves depending upon the ratio of radius to thickness was therefore drawn through the average of the test points; these curves give the compressive-buckling-stress coefficients for actual curved plates.

At high values of Z the curves approach a series of straight lines which are parallel to the theoretical curve. These straight lines are functions of r/t and may be approximated by the equation $k_x = CZ$ where C is a function of r/t expressed by the equation $C = 0.68 - 0.0005\frac{r}{t}$. This expression for C, plotted in figure 9, was obtained from experimental results given in figures 7 and 8. As Z decreases and approaches zero, the empirical curves approach the value of $k_y = 4$ which is the theoretical compressive-stress coefficiont for the buckling of flat plates with simply supported edges loaded in longitudinal compression. (See curves for simply supported plates in fig. 4.) The empirical curves of figures 7 and 8 may therefore be used to determine the compressive buckling stresses of curved plates with simply supported edges.

In order to determine the stresses that cause curved plates with clamped edges to buckle, it is necessary to modify the curves of figures 7 and 8. The longitudinal loads which cause buckling are practically independent of edge restraint at large values of Z.

(See fig. 4.) Flat plates with clamped edges loaded longitudinally will also buckle at a stress which agrees closely with the theoretically predicted value (reference 15). The curves of figures 7 and 8 are therefore modified for curved plates with clamped edges by fairing smooth transition curves between the theoretical values at low values of the curvature parameter Z and the empirical values established for the buckling of curved plates at high values of Z. The results are shown as dashed curves in figure 5.

REFERENCES

1. Leggett, D. M. A.: The Elastic Stability of a Long and Slightly Bent Rectangular Plate under Uniform Shear. Proc. Roy. Soc. (London), ser. A., vol. 162, no. 908, Sept. 1, 1937, pp. 62-83.

2. Kromm, A.: The Limit of Stability of a Curved Plate Strip under Shear and Axial Stresses. NACA TM No. 898, 1939.

3. Batdorf, S. B., Schildcrout, Murry, and Stein, Manuel: Critical Shear Stress of Long Plates with Transverse Curvature. NACA TN No. 1346, 1947.

4. Redshaw, S. C.: The Elastic Stability of a Curved Plate under Axial Thrusts. Jour. R.A.S., vol. XLII, no. 330, June 1938, p. 536.

5. Leggett, D. M. A.: The Buckling of a Long Curved Panel under Axial Compression. R. & M. No. 1899, British A.R.C., 1942.

6. Kromm, A.: Knickfestigkeit gekrümmter Platten unter gleichzeitiger Wirkung von Schub- und Längskräften. Bericht 119 der Lilienthal-Gesellschaft für Luftfahrtforschung, 1939.

7. Stowell, Elbridge Z., and Schwartz, Edward B.: Critical Stress for an Infinitely Long Flat Plate with Elastically Restrained Edges under Combined Shear and Direct Stress. NACA ARR No. 3K13, 1943.

8. Batdorf, S. B., Stein, Manuel, and Schildcrout, Murry: Critical Shear Stress of Curved Rectangular Panels. NACA TN No. 1348, 1947.

9. Cox, H. L., and Clenshaw, W. J.: Compression Tests on Curved Plates of Thin Sheet Duralumin. R. & M. No. 1894, British A.R.C., 1941.

10. Lundquist, Eugene E.: Preliminary Data on Buckling Strength of Curved Sheet Panels in Compression. NACA ARR, Nov. 1941.

11. Crate, Harold, and Levin, L. Ross: Data on Buckling Strength of Curved Sheet in Compression. NACA ARR No. 3J04, 1943.

12. Batdorf, S. B.: A Simplified Method of Elastic-Stability Analysis for Thin Cylindrical Shells. I - Donnell's Equation. NACA TN No. 1341, 1947.

13. Batdorf, S. B.: A Simplified Method of Elastic-Stability Analysis for Thin Cylindrical Shells. II - Modified Equilibrium Equation. NACA TN No. 1342, 1947.

14. Duncan, W. J.: The Principles of the Galerkin Method. R. & M. No. 1848, British A.R.C., 1938.

15. Cox, H. L.: The Buckling of Thin Plates in Compression. R. & M. No. 1554, British A.R.C., 1933.

TABLE 1

THEORETICAL COMBINATIONS OF SHEAR-STRESS AND DIRECT-AXIAL-STRESS COEFFICIENTS AND CORRESPONDING VALUES OF β^2

Z	k_x	First approximation		Second approximation		Third approximation	
		k_s	β^2	k_s	β^2	k_s	β^2
Curved plates with simply supported edges							
5	-3	7.80	0.38	7.35	0.45	7.34	0.47
	-1	6.67	.47	6.34	.52	-----	----
	1	5.34	.60	5.13	.63	-----	----
	3	3.60	.76	3.52	.78	-----	----
	4	2.35	.90	2.33	.90	-----	----
	4.76	.265	1.0	.265	1.0	-----	----
10	-4	8.95	.28	8.45	.34	8.45	.33
	-2	8.08	.30	7.63	.39	7.63	.40
	2	5.92	.41	5.67	.47	-----	----
	4	4.55	.53	4.41	.57	-----	----
	5	3.71	.60	3.62	.64	-----	----
	6	2.65	.73	2.61	.75	-----	----
	7.03	.56	.98	.56	.98	-----	----
30	-5	12.58	.10	11.94	.12	11.92	.12
	-2	11.73	.11	11.18	.12	-----	----
	5	9.58	.12	9.24	.12	-----	----
	10	7.80	.12	7.60	.12	-----	----
	15	5.67	.12	5.58	.12	-----	----
	18	3.98	.12	3.95	.12	-----	----
	21	.55	.12	.55	.12	-----	----
100	-10	21.80	.03	20.61	.04	20.61	.04
	-5	20.7	.03	19.83	.03	-----	----
	20	16.54	.03	16.04	.03	-----	----
	40	12.57	.03	12.35	.03	-----	----
	50	10.13	.03	10.04	.03	-----	----
	60	7.15	.03	7.11	.03	-----	----
	69.5	1.85	.03	1.85	.03	-----	----

TABLE 1 - Continued

THEORETICAL COMBINATIONS OF SHEAR-STRESS AND DIRECT-AXIAL-STRESS COEFFICIENTS AND CORRESPONDING VALUES OF β^2 - - Continued

Z	k_x	First approximation		Second approximation		Third approximation	
		k_s	β^2	k_s	β^2	k_s	β^2
Curved plates with simply supported edges							
300	-100	42.9	0.01	40.58	0.01	40.53	0.01
	-50	38.8	.01	36.90	.01	-----	-----
	0	34.34	.01	32.95	.01	-----	-----
	50	29.50	.01	28.58	.01	-----	-----
	100	24.10	.01	23.60	.01	-----	-----
	150	17.5	.01	17.3	.01	-----	-----
	210	1.8	.01	1.8	.01	-----	-----
1000	-200	72.0	.003	68.65	.003	68.55	.003
	0	62.6	.003	60.16	.003	60.03	.003
	200	52.0	.003	50.5	.003	50.34	.003
	400	39.5	.003	38.7	.003	-----	-----
	600	22.6	.003	22.4	.003	-----	-----
	700	3.6	.003	3.6	.003	-----	-----
Curved plates with clamped edges							
1	-5	12.78	1.03	12.11	1.2	11.91	1.23
	0	9.59	1.41	9.34	1.5	-----	-----
	1	8.88	1.50	8.66	1.6	-----	-----
	3	7.19	1.75	7.15	1.8	-----	-----
	5	5.16	2.00	5.15	2.1	-----	-----
	7	1.87	2.28	1.09	2.3	-----	-----
	7.09	0	2.30	-----	-----	-----	-----
5	-6	14.23	1.10	13.14	1.26	-----	-----
	0	10.46	1.56	10.00	1.67	-----	-----
	2	8.94	1.80	8.69	1.80	-----	-----
	4	7.20	2.07	7.12	2.08	-----	-----
	6	5.06	2.35	5.06	2.35	-----	-----
	7.5	2.73	2.58	2.47	2.60	-----	-----
	7.97	0	2.75	-----	-----	-----	-----

TABLE 1 - Concluded

THEORETICAL COMBINATIONS OF SHEAR-STRESS AND DIRECT-AXIAL-STRESS COEFFICIENTS AND CORRESPONDING VALUES OF β^2 - Concluded

Z	k_x	First approximation		Second approximation		Third approximation	
		k_s	β^2	k_s	β^2	k_s	β^2
Curved plates with clamped odges							
10	-7	17.13	1.30	14.84	1.50	-----	----
	0	12.69	1.92	11.49	2.00	-----	----
	1	11.96	2.05	10.93	2.13	-----	----
	5	8.65	2.50	8.27	2.60	-----	----
	7	6.62	3.00	6.52	2.95	-----	----
	9	4.00	3.34	3.98	3.36	-----	----
	10.14	0	3.75	-----	----	-----	----
30	-15	38.92	2.00	23.85	1.65	23.22	1.80
	0	28.23	3.32	18.44	2.65	18.10	2.75
	5	23.86	4.20	16.21	3.25	-----	----
	10	18.93	5.20	13.64	4.20	-----	----
	15	13.32	6.50	10.51	5.50	-----	----
	18	9.50	7.40	8.18	6.70	-----	----
	21	4.85	8.60	4.72	8.35	-----	----
	22.39	0	9.44	-----	----	-----	----
1000	250	105	.25	92.5	.54	-----	----
	400	97.5	.22	78	.56	-----	----
	500	90	.24	68.5	.62	62.5	1.4

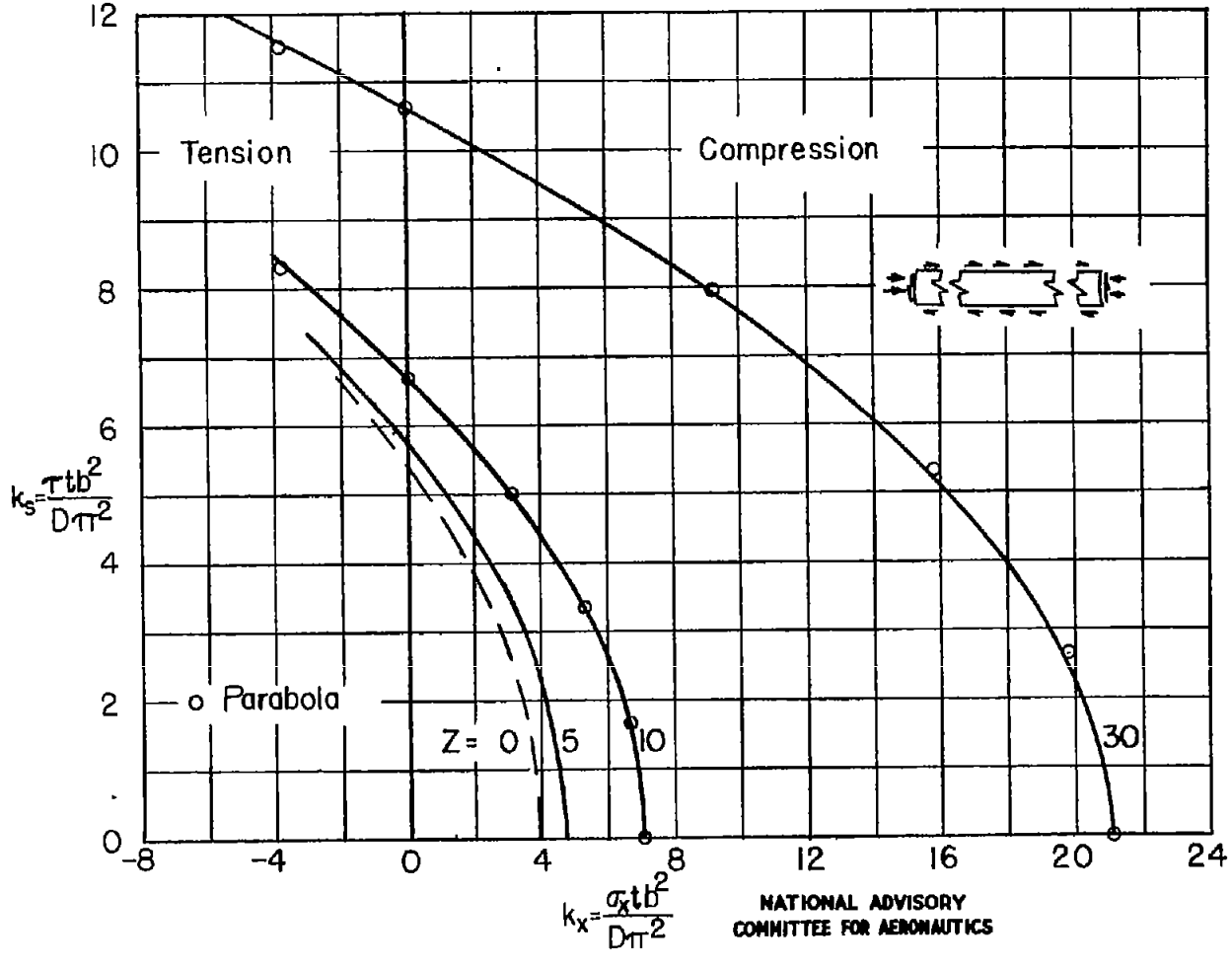

Figure 1.- Theoretical combinations of stress coefficients for long plates with transverse curvature having simply supported edges loaded in shear and direct axial stress. (Curve for Z = 0 obtained from reference 7.)

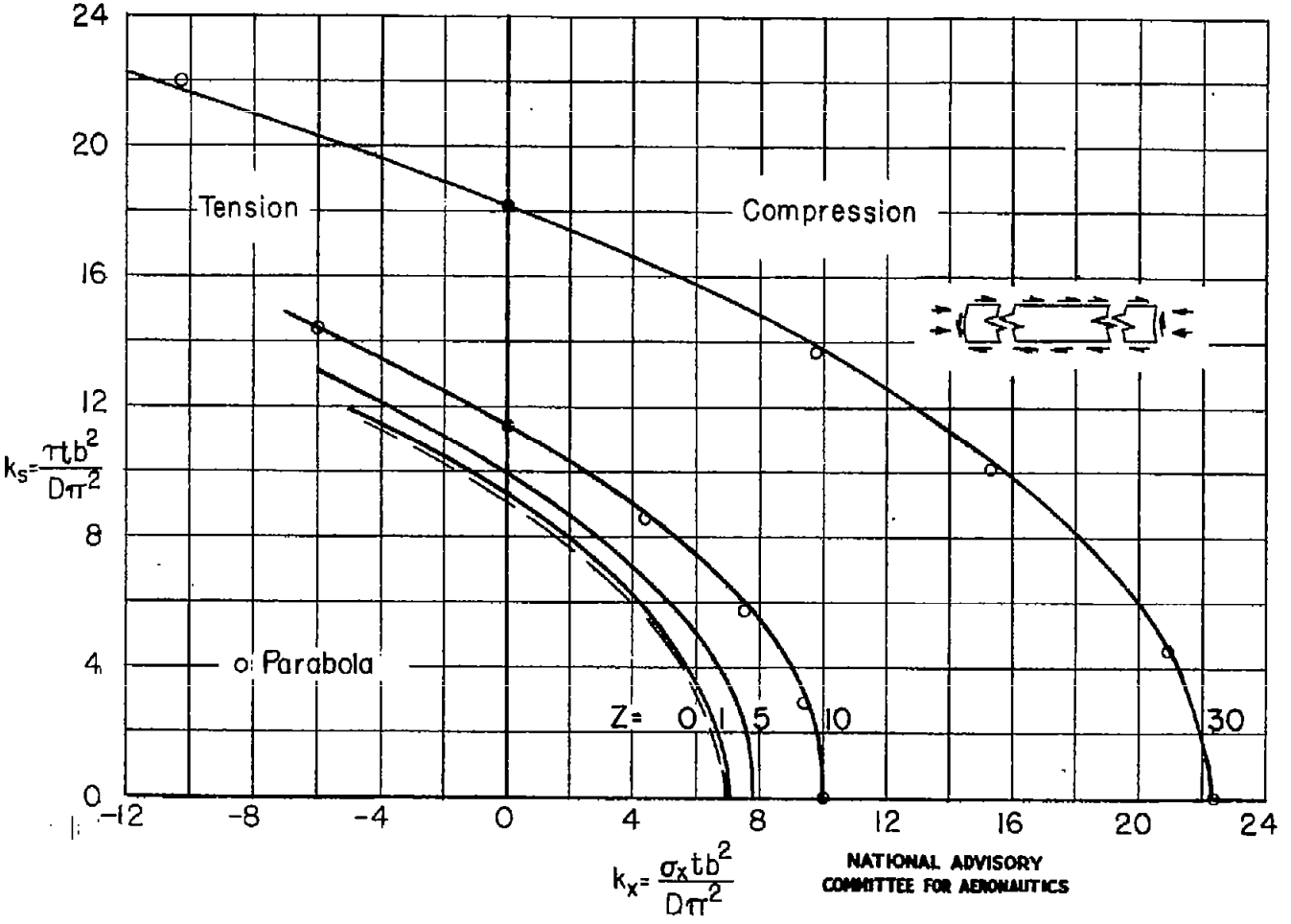

Figure 2.- Theoretical combinations of stress coefficients for long plates with transverse curvature having clamped edges loaded in shear and direct axial stress. (Curve for $Z = 0$ obtained from reference 7.)

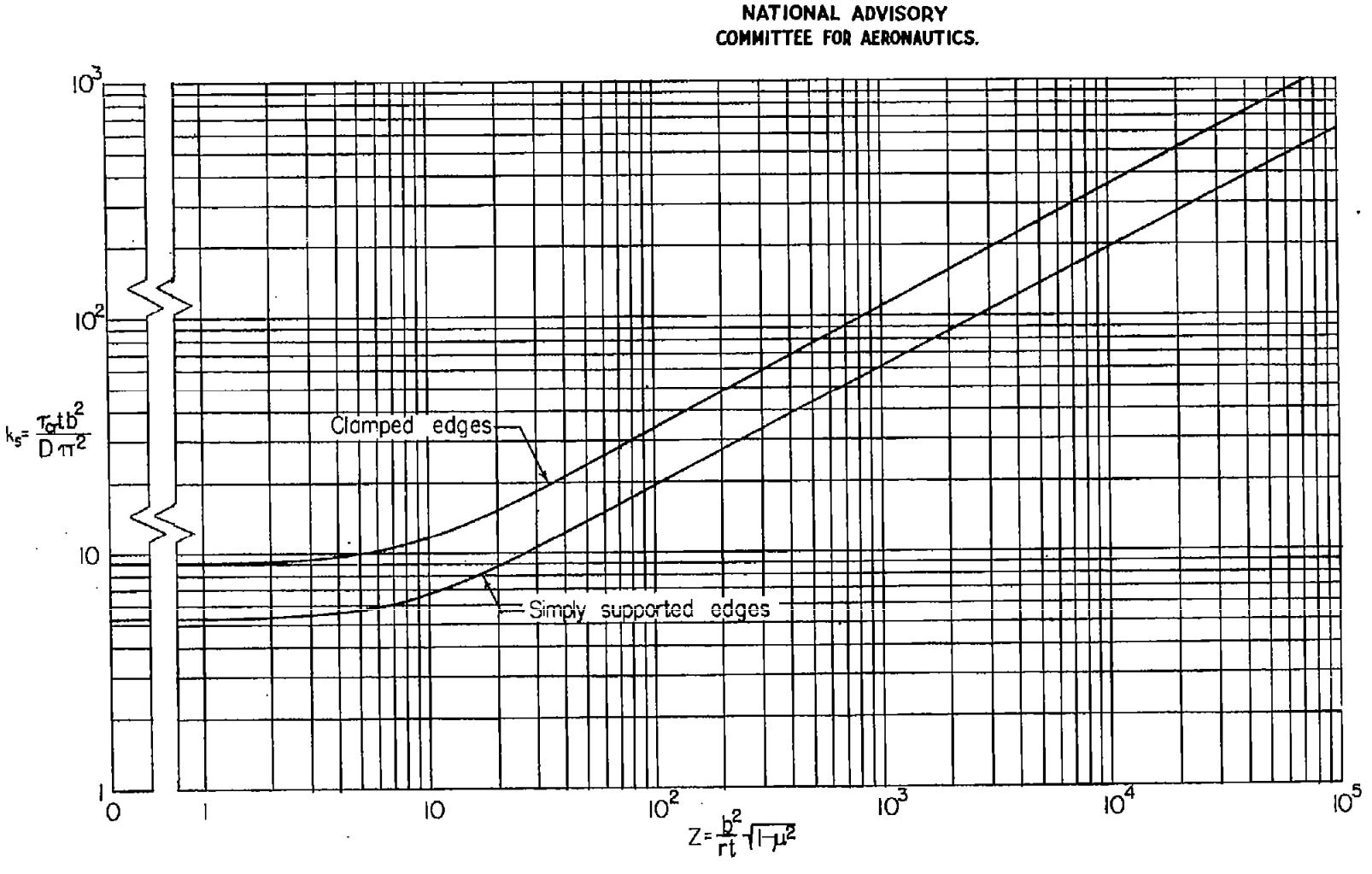

Figure 3.- Theoretical critical-shear-stress coefficients for long plates with transverse curvature having either simply supported or clamped edges.

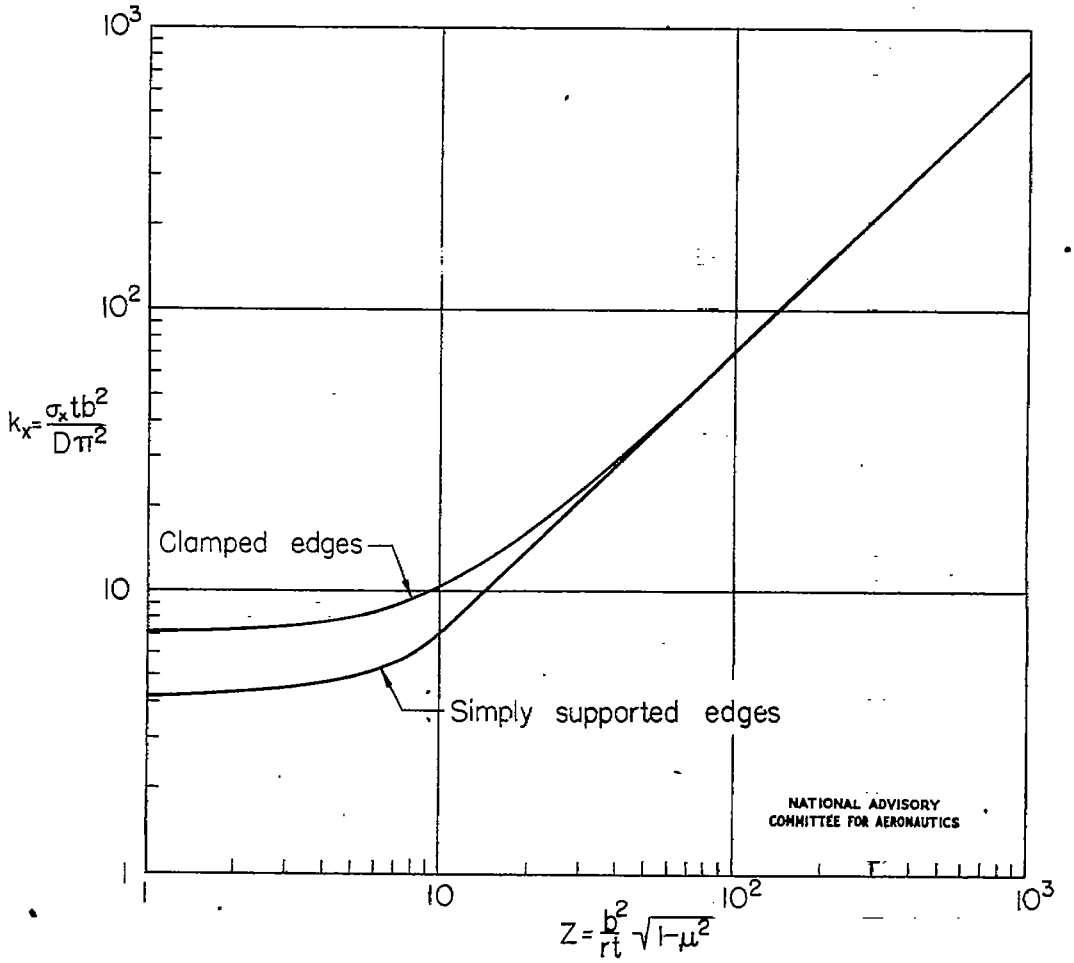

Figure 4.- Theoretical compressive-stress coefficients for long plates with transverse curvature having either simply supported or clamped edges.

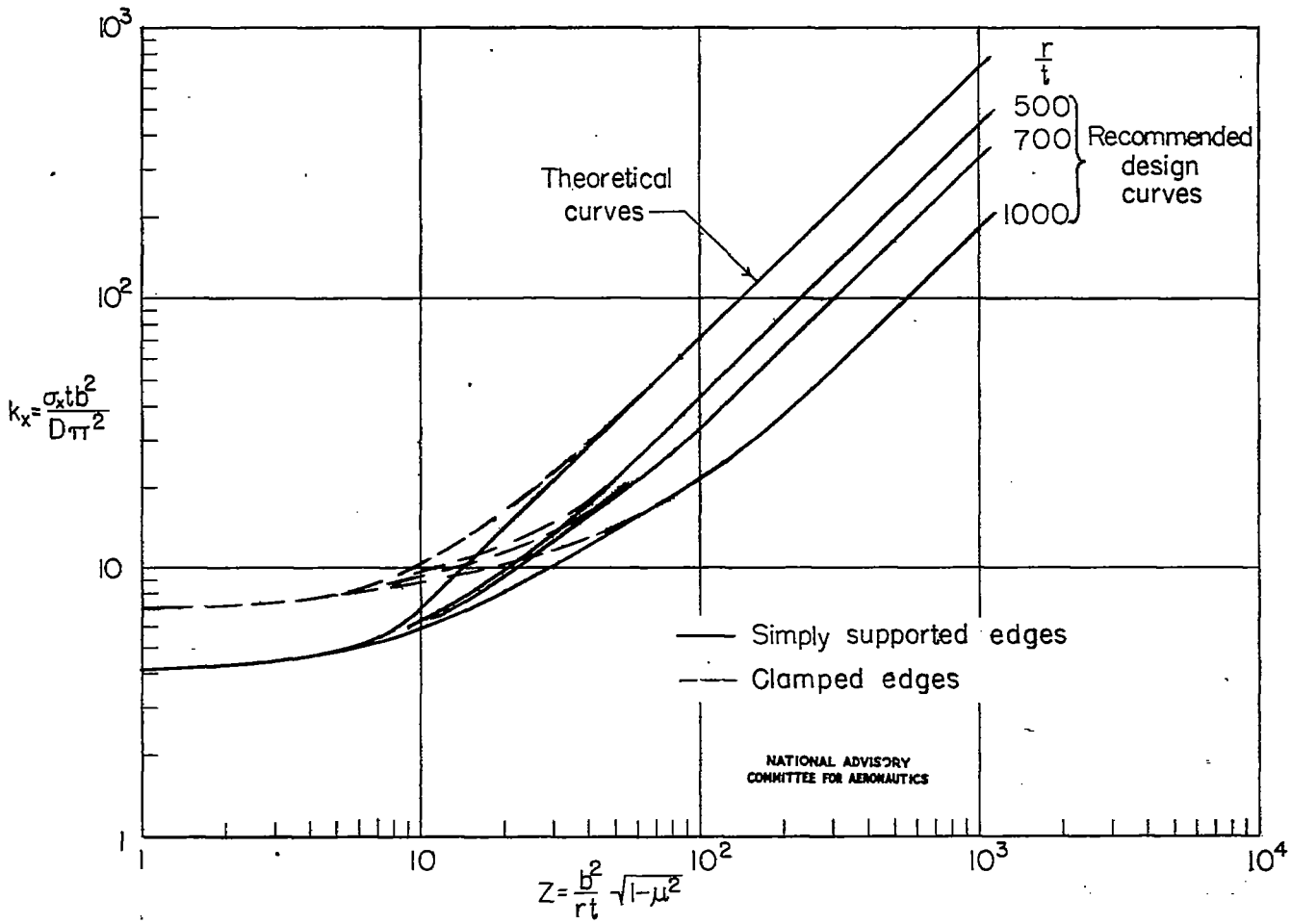

Figure 5.- Design and theoretical compressive-stress coefficients for long plates with transverse curvature having either simply supported or clamped edges.

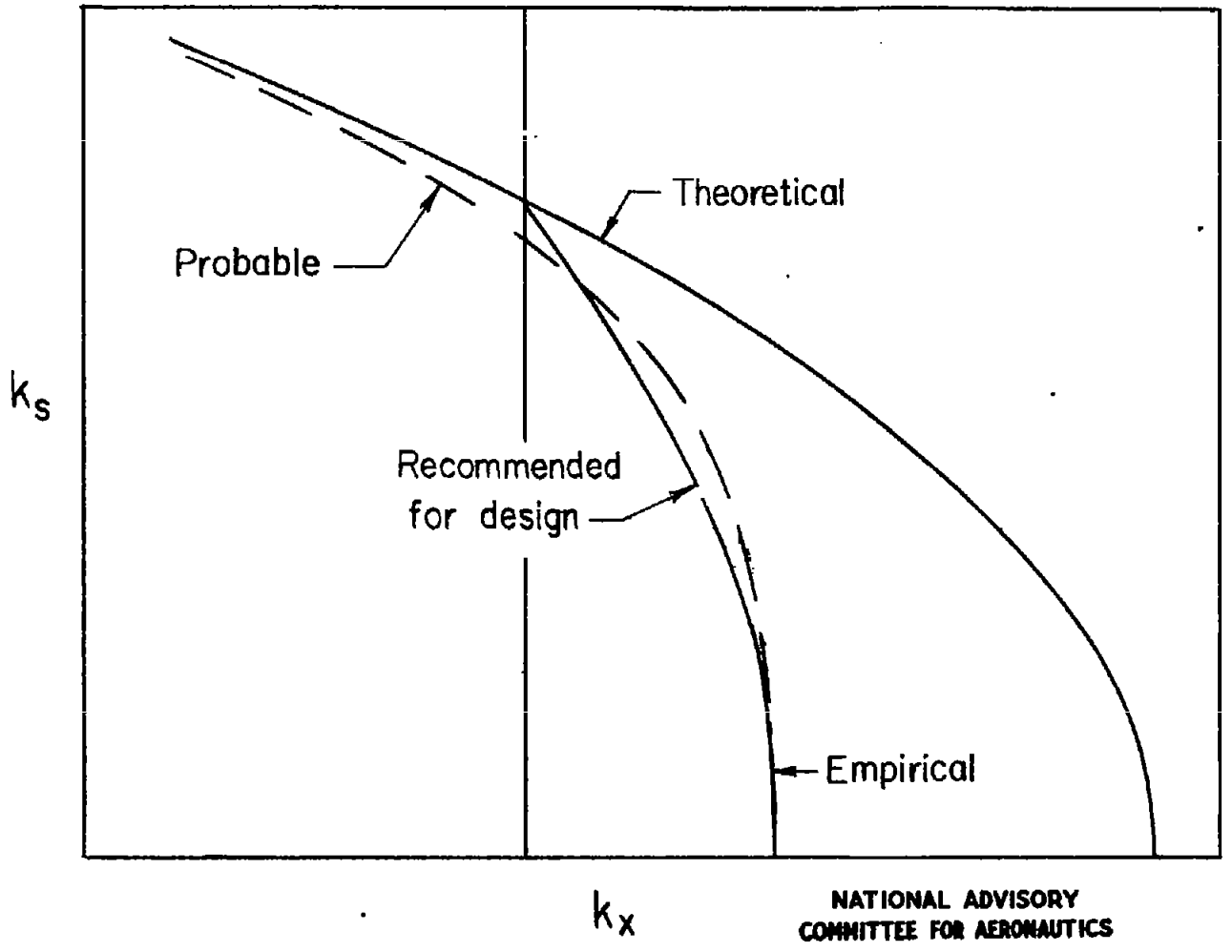

Figure 6.- Comparison of theoretical interaction curve, probable empirical interaction curve (exact location somewhat uncertain), and empirical interaction curve recommended for design of curved plates buckling under combined action of axial compression and shear.

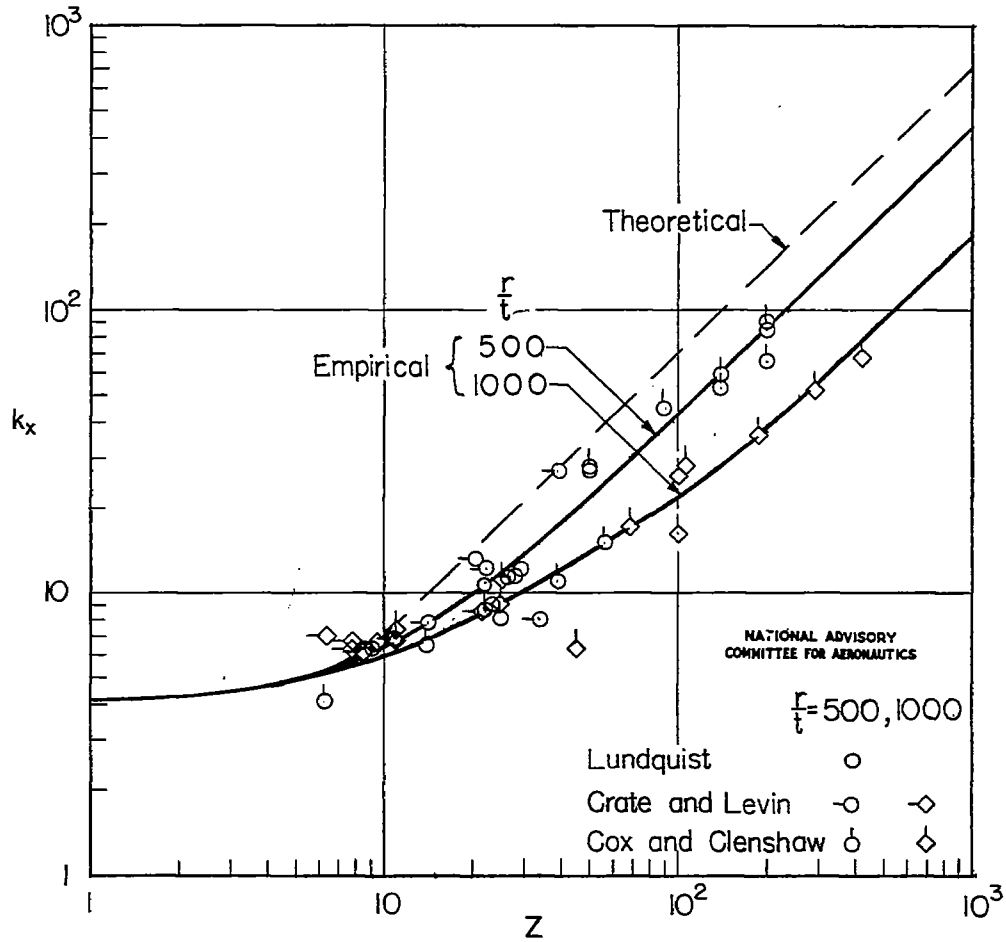

Figure 7.- Test points and design curves for plates having radius-thickness ratios of 500 and 1000 compared with theoretical curve for plates with simply supported edges loaded in axial compression.

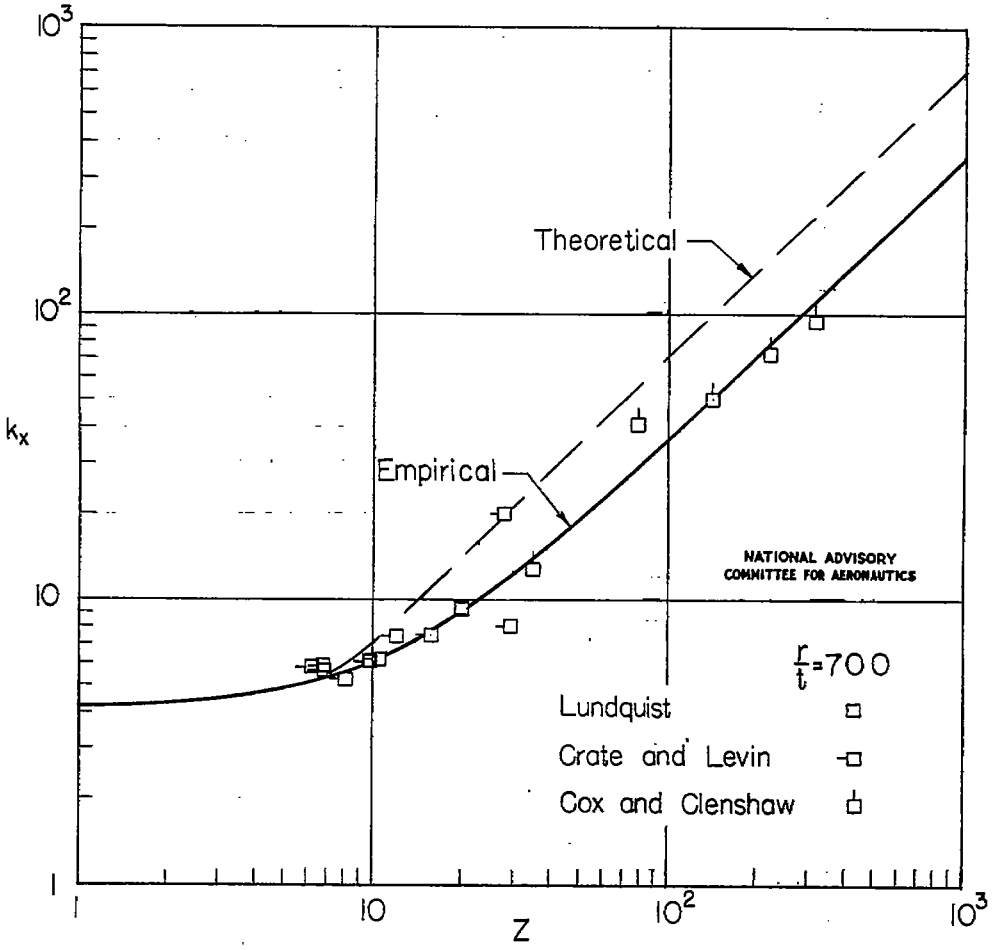

Figure 8.- Test points and design curve for plates having radius-thickness ratio of 700 compared with theoretical curve for plates with simply supported edges loaded in axial compression.

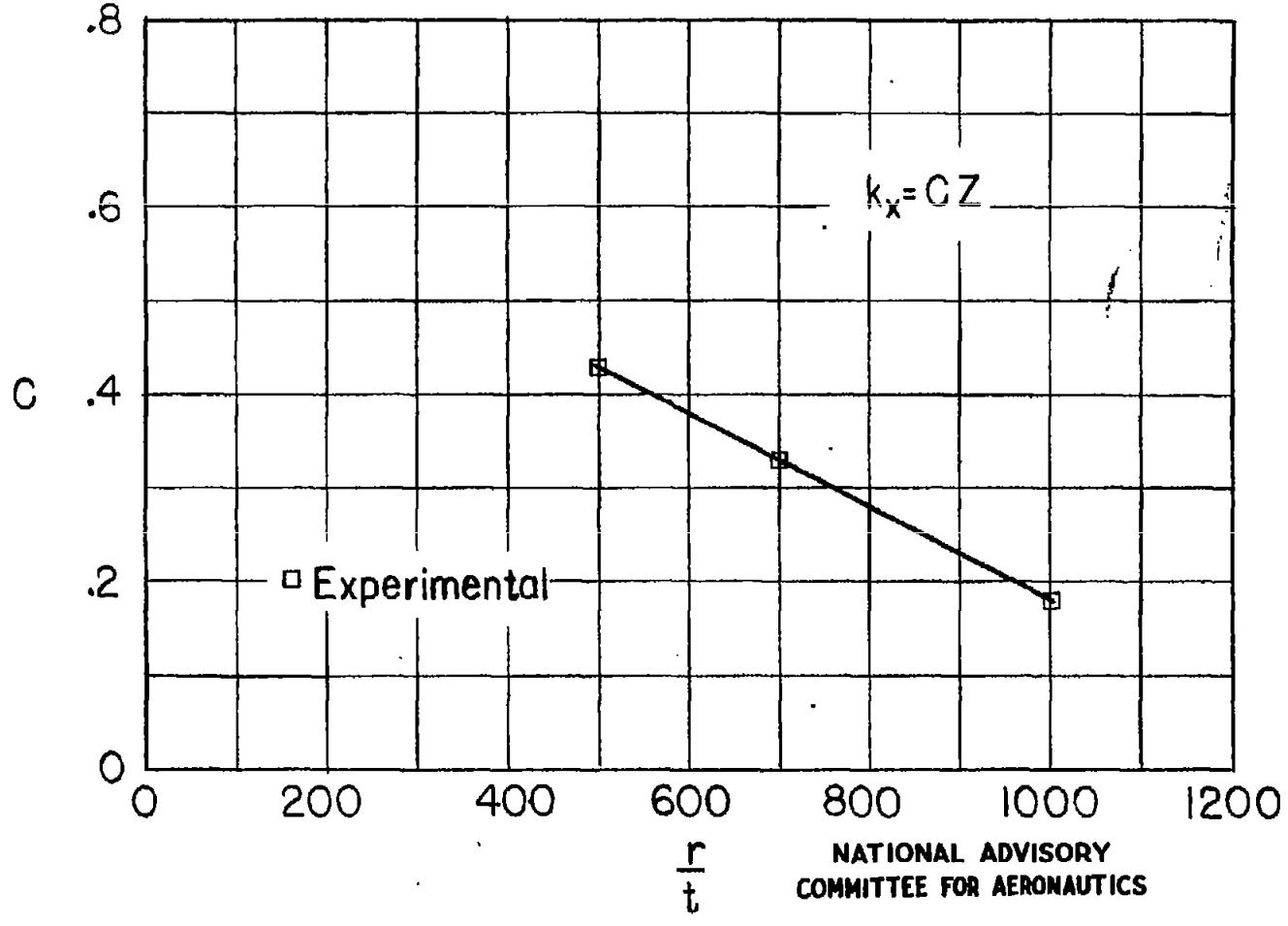

Figure 9.- Empirical coefficient for computing compressive strength of long plates with transverse curvature having moderate and high values of Z.